

Mesoporous Carbon Supported Pt-Sn-W Ternary Electrocatalyst for Membraneless Ethanol Fuel cell

M. Priya, S. Kiruthika, B. Muthukumar^{*}

Department of Chemistry, Presidency College, Chennai— 600 005, India.

Department of Chemical Engineering, SRM university, Chennai— 603 203, India.

Received 23 June 2016,

Revised 07 Sept 2016,

Accepted 10 Sept 2016

Keywords :

- ❖ Membraneless fuel cell,
- ❖ mesoporous carbon,
- ❖ Platinum, Tin,
- ❖ Tungsten,
- ❖ Ethanol

priyamanokhar@gmail.com

Tel.: +91-44-28544894

Abstract

In this work represent electronic effect brought with the addition of W contributes to higher catalytic activity of Pt–Sn–W/MC catalyst for ethanol oxidation in membraneless ethanol fuel cell (MLEFC). Pt₁₀₀/MC, Pt₈₀Sn₂₀/MC, Pt₉₀W₁₀/MC and Pt₈₀Sn₁₅W₀₅/MC catalysts were synthesized by thermal decomposition of polymeric precursor method. The particle size and lattice parameter of the catalysts were determined by means of X-ray diffraction. Transmission electron microscopy of all catalysts showed a good distribution of the particles on the mesoporous carbon support voltammetry and chronoamperometric results obtained at room temperature showed that Pt–Sn/MC, Pt–W/MC and Pt–Sn–W/MC displayed better catalytic activity for ethanol oxidation compared to Pt/MC. The performance of the Single cell test shows that ternary based Pt₈₀Sn₁₅W₀₅/MC produces maximum power density and current density compared to all the prepared catalyst in membraneless ethanol fuel cell. The polarization graph also shows that cell performance increased the addition of the W to the Pt–Sn catalyst.

1. Introduction

Energy is the foundation of economic growth, researchers have been accomplishing efforts to develop elevated efficiency employ of energy assets. In recent years, considerable attention has been devoted to certain direct energy-conversion devices, notably fuel cells, which find a way around the intermediate step of conversion to heat energy in electrical power generation. Fuel cells one of best and alternative technology for energy production devices which convert chemical energy stored in fuel and oxidant straightly into electrical energy [1]. Fuel cells have a higher energy density than batteries. The widespread use of portable electronic devices stimulates the rapid development of miniature power sources. Among them, micro fuel cells become more and more attractive due to their advantages of high energy-conversion efficiency, and capability of producing electricity as long as fuel and oxidant are supplied to the electrodes. The membraneless micro fuel cell is one of the new technologies in fuel cell area. This type of fuel cell is considered as a prospective power sources for portable devices in which liquid fuel and oxidant are used as an energy sources. At present, the proton-exchange membrane fuel cell (PEMFC) and the direct methanol fuel cell (DMFC) are considered as candidates for portable micro fuel cells. However, PEMFCs and DMFCs both rely on a membrane and there are several problems associated with their operation that include, membrane dry out, fuel crossover of reactants, water management and carbon monoxide production that could potentially poison the catalyst. Based on these limitations, several compounds were investigated as possible fuels for MLFCs. Although ethanols emerge as the most attractive and promising option to overcome the problems detected in DMFCs [2-4]. Ethanol has a higher theoretical mass energy density than methanol (8.0 vs. 6.1 kWh kg⁻¹), and it is known that ethanol is non-toxic for humans, it is naturally available and it can be easily renewed by the fermentation of sugar-containing agricultural biomass [5,6]. However, to oxidize ethanol efficiency it is necessary to develop a catalyst capable of converting it completely to CO₂. The novel catalyst should be able to break the C–C bond of ethanol molecule and to eliminate the adsorbed intermediate CO-like [7]. Although platinum has been recognized to be the most active catalyst for ethanol oxidation [8]. Nevertheless, at normal temperature pure platinum is not a extremely fine anode catalyst for ethanol oxidation, since it is rapidly poisoned by the strongly adsorbed intermediates such that CH₃COOH, CH₄, CH₃CHO and CO, among which CO_{ads} is constantly measured as one of the major poisoning group at normal operating temperature. Recent studies have shown that bimetallic Pt-based catalysts can enhance the oxidation of ethanol molecules due to the bifunctional or electronic effects or the combination

of both effects. A second transition metal (M) such as Ru, Sn, Mo, Rh, Os etc) can have been introduced as co-catalyst in the Pt surface [9-11] among them Pt–Sn is best anode catalyst can be found in the literature. It is due to adding of Sn improved the catalytic effect of platinum through the bifunctional mechanism and electronic effects. These two effect combine together influence the density of electronic states of Pt, enhances to weakening of Pt–CO bonds [12-15]. To date, several publications on trimetallic systems that reported encouraging results [16-18].

Recently works demonstrate that mesoporous carbon, xerogels, aerogels, graphene, ordered mesoporous carbon, and carbon nanocoil used as the supporting materials. Rao et al. [19] investigated the consequence of carbon porosity on the specific performance of the Pt–Ru/C catalyst for methanol oxidation in fuel cell reaction. Figueiredo et al [20] suggested that carbon supports materials have high concentration of oxygen-containing surface groups increased the catalytic activity. Furthermore Arbizzani et al. [21] demonstrate that Pt–Ru supported on a mesoporous carbon given the better performance catalysts. Among them, mesoporous carbon is used as the support material best activity for fuel cell reaction. Although mesoporous carbon (MC) modified arrangement has been used as support for catalysts exhibiting higher performance. It is due to high electrical surface area, a good electrical conductivity, a high number of ordered mesoporous carbon.

In this present study, Pt, Pt–Sn and Pt–Sn–W electrocatalysts supported on mesoporous carbon were synthesized by thermal decomposition of polymer precursor synthetic methods. The prepared catalysts are characterized by dispersive X-ray spectroscopy (EDX), transmission electron microscopy (TEM), X-ray diffractometry (XRD) and electrochemical characterization techniques of cyclic voltammetry (CV), and chronoamperometry (CA). The catalytic activity of the prepared catalysts toward ethanol oxidation has been evaluated in a membraneless ethanol fuel cell (MLEFC) as the anode catalysts.

2. Experiment

2.1 Materials

The precursors used for preparation of electrocatalysts were $\text{H}_2\text{PtCl}_6 \cdot 6\text{H}_2\text{O}$, $\text{SnCl}_2 \cdot 2\text{H}_2\text{O}$, $\text{WCl}_6 \cdot x\text{H}_2\text{O}$ and mesoporous carbon as support. Graphite plates (3 cm long and 0.1 cm wide, from E-TEK) were used as substrates for catalyst to prepare the electrodes. Deionized water (DI) (from Merck) was used as the solvent; Nafion[®] (DE 521, DuPont USA) dispersion was used to make the catalyst slurry. Ethanol (from Merck), sodium perborate (from Riedel) and H_2SO_4 (from Merck) were used as the fuel, the oxidant and as the electrolyte for electrochemical analysis, respectively; all the chemicals were of analytical grade. Pt/MC (40-wt%) was used as the cathode catalyst.

2.2 Preparation of catalysts

Pt–Sn–W/MC is prepared by thermal decomposition of a polymeric precursor method. The polymeric metal precursors were dissolved in isopropanol separately. Then, citric acid (CA) (Merck) was mixed with ethylene glycol (EG) (Merck) was mixed with ethylene glycol (EG) (Merck) at 60–65°C. The metal precursor (H_2PtCl_6 or $\text{WCl}_6 \cdot x\text{H}_2\text{O}$ (Aldrich) 0.1 mol dm⁻¹ solution dissolved in isopropanol was then added to this mixture to give CA: EG: M molar ratios of 1:4:0.25 for M=Pt and M=W, respectively and followed by vigorous stirring for 2-3 h. The Sn polymeric precursor was also prepared in a similar way, but the molar ratio CA: EG: TC was 3:10:1, where TC is tin citrate, prepared as described elsewhere [22]. When (mesoporous carbon), which had been previously treated for 4 h at 400°C under nitrogen atmosphere, was added to the precursor mixture, to obtain a catalysts loading of 40wt%. This mixture was finally dispersed in ethanol by ultrasonication for 10 min. thermal treatment was carried out in a tubular oven under a nitrogen atmosphere. Finally, after being cooled to room temperature, the catalysts were again kept in an oven under air atmosphere at 400°C for 1h to eliminate the excess organic carbon.

2.3 Physical and Chemical Characterization

The X-ray diffraction (XRD) analyses are used to find out crystal structure of the prepared catalyst was characterized by powder X-ray diffraction using a Rigaku multiflex diffractometer (model RU-200 B) with $\text{Cu-K}_{\alpha 1}$ radiation source ($\lambda_{\text{K}\alpha 1} = 1.5406\text{\AA}$) operating temperature. The tube current was 40 mA with a tube voltage 40kV. The 2θ angular regions between 20° and 90° were recorded at scan rate of 5° min⁻¹. The crystallite size was found out Scherrer's equation. The composition ratios were finding by energy-dispersive X-ray (EDX) method using an integrated TEM (Transmission Electron Microscope) instrument. The particle size of the prepared catalyst is observed by TEM.

Electrochemical measurements were carried out using the thin porous coating technique [23]. The working electrode were prepared to amount of 20 mg of the electrocatalysts was added to a solution of 50 ml of water

containing three drops of 6% polytetrafluoroethylene (PTFE) suspension. The mixture was treated in an ultrasound bath for 10 min and transferred to the cavity of working electrode. In cyclic voltammetry and chronoamperometry experiments, the current values (*I*) were expressed in amperes and were normalized per gram of platinum. The quantity of platinum was calculated considering mass of the electrocatalyst present in the working electrode multiplied by its percentage of platinum. Cyclic voltammetry and chronoamperometry experiments were performed at 25°C with 1 M ethanol in 0.5 M H₂SO₄ solution saturated with N₂ gas was purged with high-purity nitrogen gas for at least 30 minutes to ensure oxygen-free measurement. The entire electrochemical studies were performed on an electrochemical workstation (CH instruments, model CHI6650, USA) interfaced with a personal computer using the CHI software, at room temperature. A regular three-electrode electrochemical cell by cyclic voltammetry (CV) and chronoamperometry (CA) technique was used for measurements. Catalyst coated glass carbon electrode (GCE, 3 mm diameter and 0.071 cm² of electrode area, from CHI, USA) was used as the working electrode. Ag/AgCl in saturated KCl was used as reference electrode (RHE).

3. Results and discussion

3.1 X-ray diffraction (XRD)

Figure 1 illustrates the XRD pattern of Pt/MC (100), Pt–Sn/MC (80:20), Pt–W/MC (90:10) and Pt–Sn–W/MC catalysts. The diffraction peaks seen in all the diffraction patterns at around 25–35° are associated with (0 2 2) mesoporous carbon support [24]. The diffraction peaks at around 39°, 46° and 68° are attributed to Pt (1 1 1), (2 0 0) and (2 2 0) planes, respectively which represents the typical character of crystalline Pt which face centered cubic (FCC) crystalline structure. Figure shows a slight shift in Pt peak position for the catalysts containing Sn, which are shifted to lower 2θ values when compared with pure Pt XRD pattern. Addition of W in the binary Pt–W/MC catalysts results in a shift of the diffraction peaks of Pt to higher 2θ values. This suggests that there is also formation of a solid solution between Pt and W.

The presence of WO_x in the ternary Pt–Sn–W/MC and binary Pt–W/MC catalysts is not observed in the XRD pattern. However, their presence cannot be ruled out because they may be present in small amounts and amorphous forms.

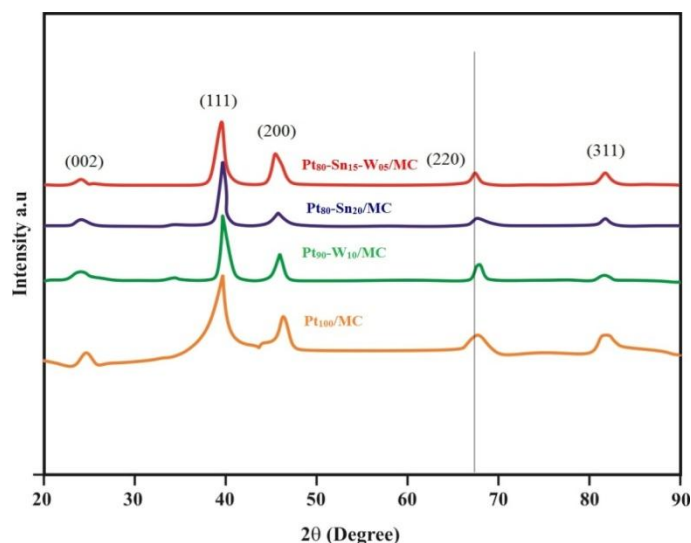


Figure 1: XRD patterns for the prepared catalysts a) Pt/MC (100), b)Pt–Sn/MC (80:20), c)Pt–W/MC (90:10), and d) Pt–Sn–W/MC (80:15:05).

Table 1 represent lattice parameters of Pt/MC, Pt–Sn/MC, Pt–W/MC and Pt–Sn–W catalysts, which reveal the formation of alloy catalysts and can be calculated by using the Pt (2 2 0) crystal face, are specified. The lattice parameters acquired for the Pt–W catalyst are smaller than Pt/MC. Pt–Sn/MC and Pt–Sn–W/MC catalysts are larger than Pt/MC. It is suggest that, the decrease in lattice parameters of the alloy catalysts reveal enlarge in the inclusion of Sn and W into alloyed state. The mean particle size *d* may be predictable from the Pt (200) corresponding to Debye-Scherrer formula.

Table 1: Characterization parameters for the Pt/MC (100), Pt–Sn/MC (80:20), Pt–W/MC (90:10) and Pt–Sn–W/MC (80:15:05) catalysts.

Electrocatalyst	Nominal atomic ratio			EDX Atomic ratio			Lattice parameter (nm)	2θ	Crystallite size (nm)
	Pt	Sn	W	Pt	Sn	W			
Pt/MC	100	-	-	-	-	-	0.3916	-	-
Pt–Sn/MC	80	20	-	79	21	-	0.3934	67.71	7.8
Pt–W/MC	90	-	10	87	-	13	0.3911	67.48	12.8
Pt–Sn–W/MC	80	15	05	70	22	8	0.3917	67.57	7.4

3.2 Energy dispersive X-ray spectroscopy (EDX)

Chemical composition of Pt/MC, Pt–Sn/MC, Pt–W/MC and Pt–Sn–W/MC, catalysts is evaluated by EDX experiments. The EDX experiments depict that determined composition is relatively similar to the theoretical value. H_2PtCl_6 , $SnCl_3$ and WO_3 as precursors were completely reduced to Pt, Sn and W metals, correspondingly. Figure.2 shows EDX model of Pt–Sn–W/MC and Pt–Sn/MC catalysts. Characteristic standards of the composition analysis of them are represented in table 2.

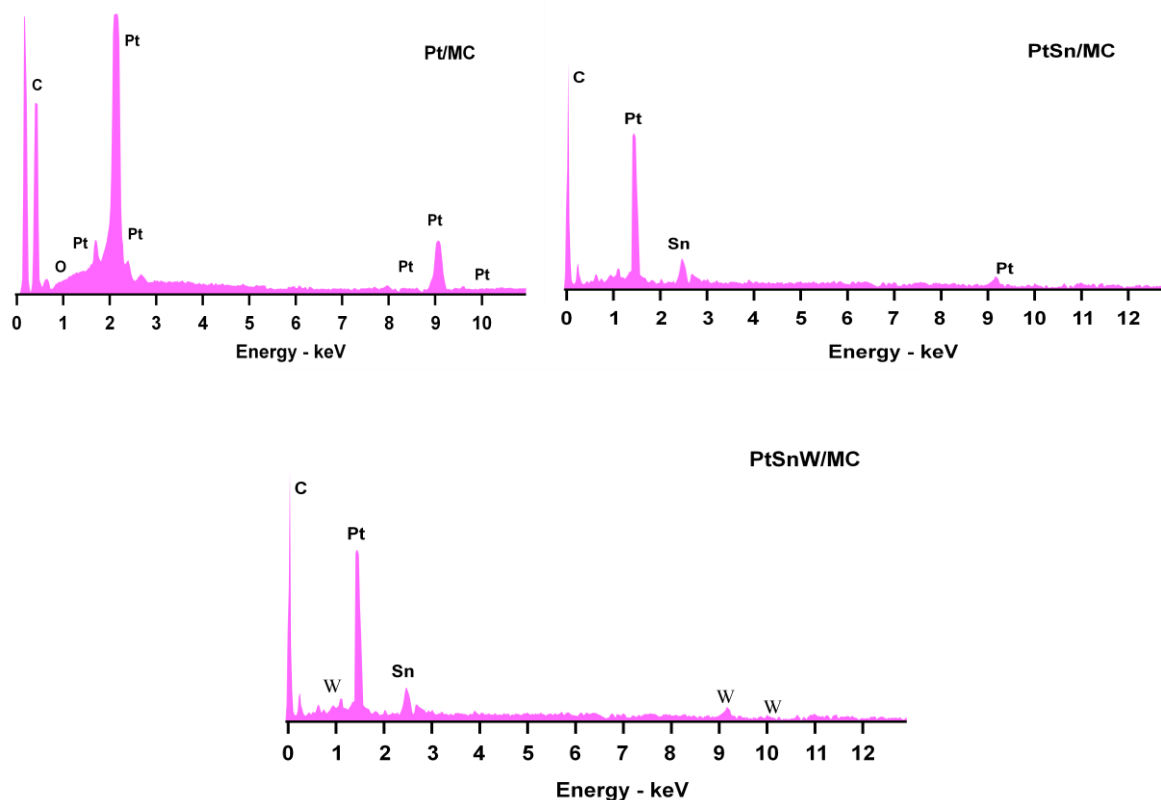


Figure 2: EDX spectra of Pt/MC (100), Pt–Sn/MC (80:20) and Pt–Sn–W/MC (85:15:05) catalysts.

3.3 Transmission Electron Microscopy (TEM)

The TEM image in Figure 3a-d of the catalysts prepared shows that spherical like nanoparticles of catalysts are uniformly distributed over carbon support. The lighter particles of 30-50 nm size are carbon supports. The average particle size for Pt–Sn–W/MC (80:15:05) is smaller (7.4 nm) than the binary catalysts such as Pt–W/MC (90:10) and Pt–Sn/MC (80:20) was 12.8 and 7.8. Figure 4 represent the average value of the particle diameter distribution histograms. The addition of W seemed to facilitate the dispersion of PtSn particles on the mesoporous carbon support and reduced the particle size.

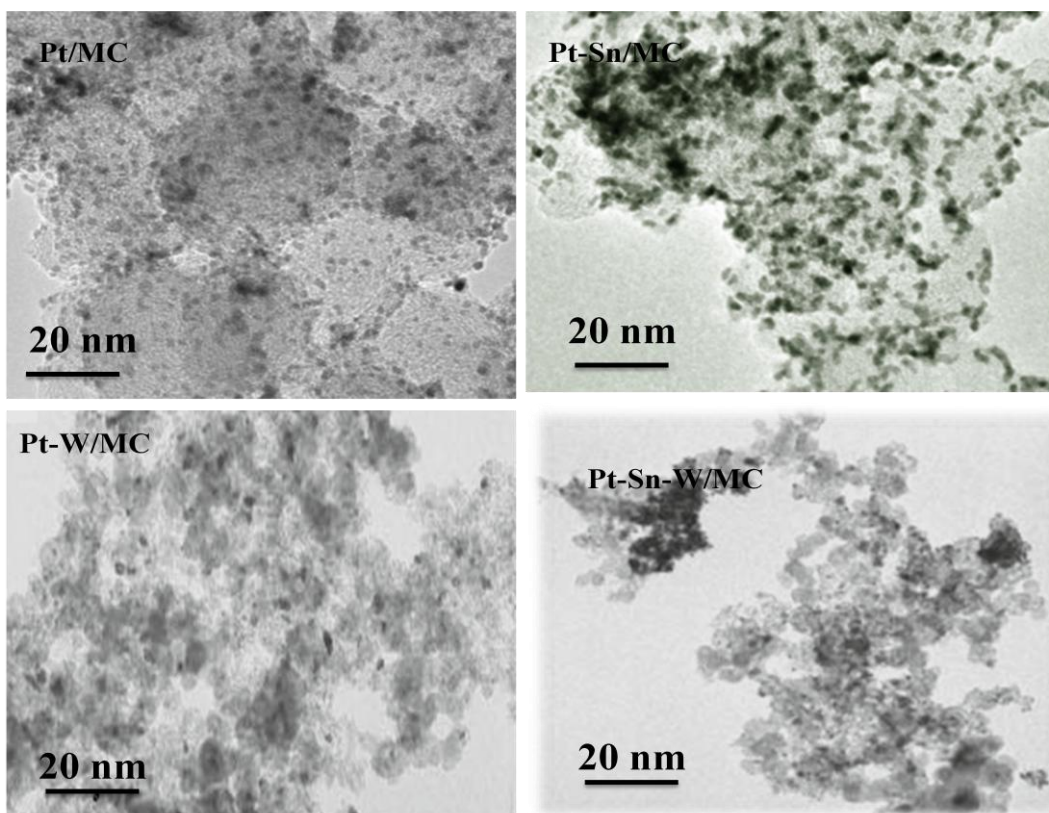


Figure 3: TEM images of a) Pt/MC(100), b) Pt–Sn/MC(80:20),c) Pt–W/MC (90:10) and d) Pt–Sn–W/MC (80:15:05) catalysts.

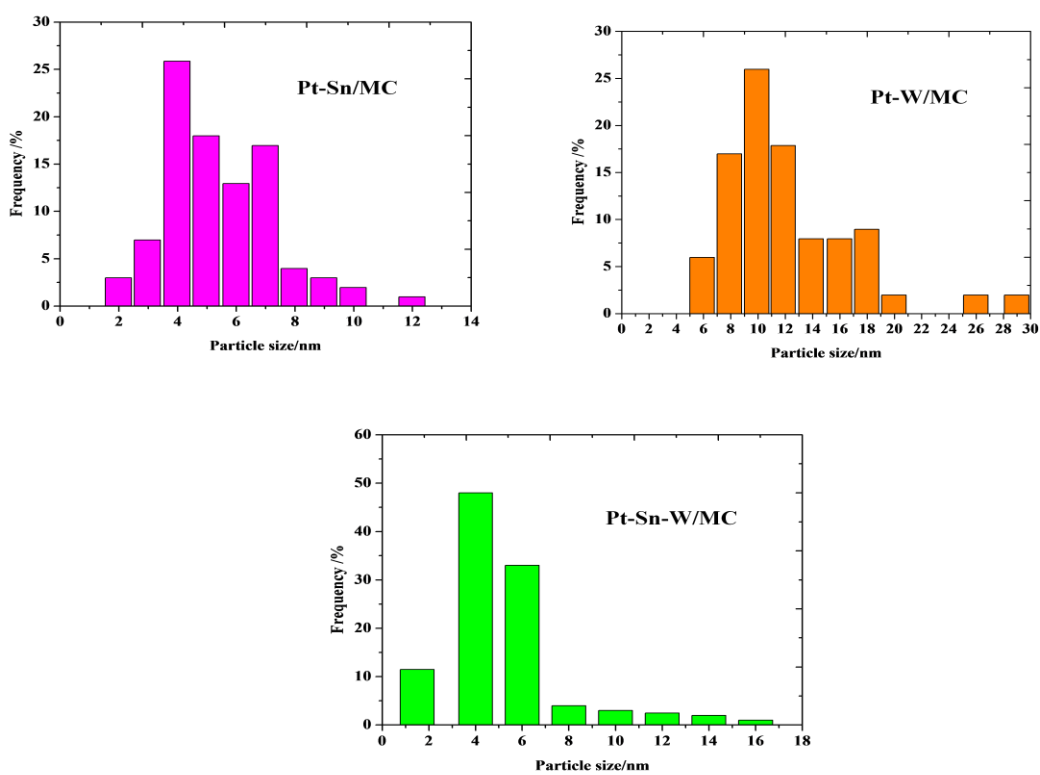


Figure 4: TEM particle size distribution of Pt–Sn/MC (80:20), Pt–W/MC (90:10) and Pt–Sn–W/MC (80:15:05) catalysts.

3.4 Cyclic voltammetry

Figure 5a. Shows representative cyclic voltammograms obtained for the Pt–Sn–W/MC electrocatalysts. The hydrogen adsorption/desorption region (0.0–0.4 V vs. RHE) is poorly defined, and the current in the double layer region (0.4–0.8 V vs. RHE) is higher compared with that of the pure Pt-catalyst. This behavior is characteristic of supported carbon electrocatalysts containing transition metals [25]. Taking the Pt/MC composition as reference, the binary Pt-catalyst incorporated with Sn or W has a voltammetric charge similar to that of the pure Pt catalyst. However, when both metals are simultaneously added to Pt to form ternary catalysts (Pt–Sn–W/MC), a considerable increase in the voltammetric charge is observed. Comparing the Pt/MC, Pt–Sn/MC, Pt–W/MC and Pt–Sn–W/MC catalysts, addition of W into bimetallic Pt–Sn/MC enhances a development of the ionic charge.

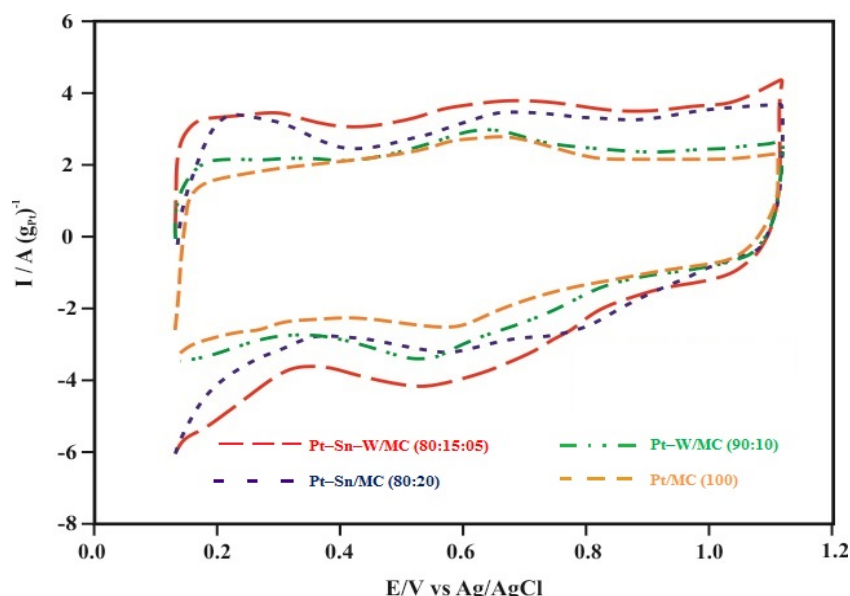


Figure 5a: Cyclic voltammograms for ethanol oxidation for Pt–Sn/MC (80:20), Pt–W/MC (90:10) and Pt–Sn–W/MC (80:15:05) in 0.5 M H₂SO₄ solution at normal temperature.

Figure 5b shows the cyclic voltammograms (CV) of ethanol oxidation under acidic conditions (1.0 M C₂H₅OH and 0.5 M H₂SO₄) catalyzed by Pt–Sn/MC (80:20), Pt–W/MC (90:10) and Pt–Sn–W/MC (80:15:05) catalysts. All the current values were normalized by the geometric surface area of the electrode used. At a first glance, the ethanol oxidation at geometric surface area of the electrode used. At a first step, represent the ethanol oxidation on Pt-based catalysts beings at -0.25V versus Ag/AgCl. The ethanol oxidation onset potential is about 0.2 V lower than that obtained with pure Pt/MC. The main results of CV test of Pt–Sn/MC (80:20), Pt–W/MC (90:10), and Pt–Sn–W/MC (80:15:05) catalysts are listed in table 2 including the positive peak potentials and corresponding peak current densities of ethanol electrooxidation. As already known [Vigier et al 2004, Calegario et al 2006], pure Pt/MC catalyst (figure) does not behave as a very good anode for ethanol electrooxidation due to its poisoning by strongly adsorbed intermediates such as CO. At this point, the better activity obtained from the ternary electrocatalysts could be explained by interaction of the beneficial synergistic effect. In fact, as observed in figure, the introduction of Sn and/or W leads to an increase in the electro-activity of the binary and ternary electrocatalysts compared to pure Pt/MC. The performance of Pt–Sn–W/MC catalyst for ethanol among Pt–Sn and W and mesoporous carbon (MC). The charge promoted by the introduction W and MC in the crystalline structure lead to the increase in the number of exposed active sites which was observed by the hydrogen adsorption and desorption current of different catalysts in CVs. This must indicate an increase in structural defects or roughness, making the ternary electrocatalysts better candidates for such catalytic process [26]. It is seen in figure that the onset potentials of ethanol electro-oxidation for Pt/MC, Pt–Sn/MC and Pt–W/MC are at about 0.4V. While for tri-metallic catalysts Pt–Sn–W/MC onset potentials ethanol electro-oxidation is earlier at about 0.2V, i.e. shifted to negative potential by 200 mV. It is seen in Fig and table that the shifted in oxidation peak to negative potential is highest in case of Pt–Sn–W/MC and appears at about 0.79 V (vs. Ag/AgCl). The peak potential on the Pt–Sn–W/MC catalyst during positive potential scanning is ~ 20 mV lower than that for the Pt–Sn/MC and Pt–W/MC catalysts. Although the peak current density for Pt–Sn–W/MC catalyst is 6.3 and 3.2 mA/cm² higher than the Pt–Sn/MC and Pt–W/MC catalysts respectively. As a result, the

performance of Pt–Sn–W/MC catalyst for ethanol electrooxidation is much better than that for the Pt–Sn/MC and Pt–W/MC catalysts.

In support of ethanol oxidation on bimetallic Pt–Sn/MC, Pt–W/MC and trimetallic Pt–Sn–W/MC shown two curves through the positive scan can be attributed to ethanol oxidation reaction as follows [27]:

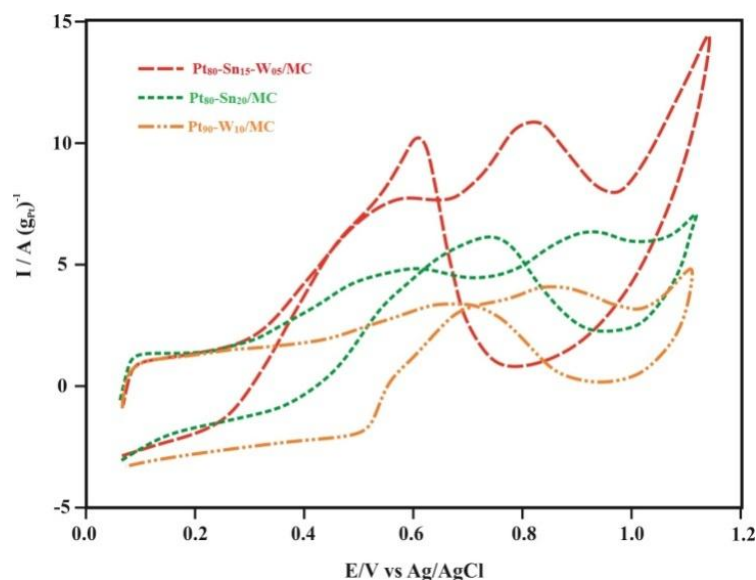
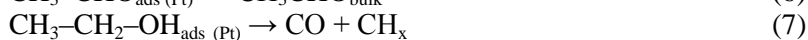
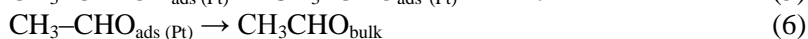
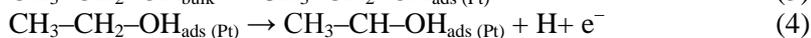


Figure 5b: Cyclic voltammograms of Pt–Sn/MC (80:20), Pt–W/MC (90:10), and Pt–Sn–W/MC (80:15:05) electrocatalysts in 0.5 M H₂SO₄ + 1.0 M ethanol at room temperature with a scan rate of 50mV/s.

At higher potentials (< 0.4 V) mechanism can be explained from Eqs. 8-11 i.e. interfacial water activation occurs resulting OH-species with facilitate formation of high oxidation state compounds acetic acid and CO₂. The addition of a co-catalyst shifts water direct oxidation of adsorbed ethanol to form acetic acid.

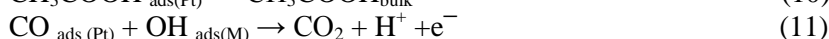
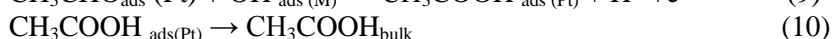
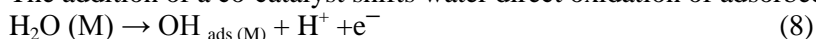


Table 2: CV results of Pt/MC (100), Pt–Sn/MC (80:20), Pt–W/MC (90:10) and Pt–Sn–W/MC (80:15:05) electrocatalysts at room temperature.

Catalyst	Scan rate 50 mV/s	
	Positive peak potential (mV vs. Ag/AgCl)	Peak current density (mA/cm ²)
Pt/MC (100)	0.75	3.2
Pt–Sn/MC (80:50)	0.75	6.3
Pt–W/MC (90:10)	0.78	9.8
Pt–Sn–W/MC (80:15:05)	0.79	11.21

3.5 Chronoamperometry

The Pt/MC, Pt–Sn/MC, Pt–W/MC and Pt–Sn–W/MC electrocatalysts performances for ethanol oxidation were studied by chronoamperometry (CA) at 0.5 V vs Ag/AgCl for 2 h to evaluate both the electrocatalytic activity of the catalysts and the poisoning of the active surface under continuous operation conditions. Figure.6 shows the

representative chronoamperograms obtained for the different electrocatalysts whose current densities were normalized by Pt mass. During the first 5 min, a sharp decrease in the current density. The occurrence of a bifunctional mechanism in which Pt affects ethanol adsorption and dissociation, while tin affects ethanol adsorption and dissociation, while tin and W provides oxygenated species at lower potential for the oxidative removal of the adsorbed intermediates formed during ethanol oxidation. This assumption is in agreement with earlier results [28,29], which claim that the bifunctional mechanism could be favored by a synergetic effect between the W and Sn sites. A change in the platinum electronic density associated with the formation of alloys of Pt, Sn and/or W. This could modify the ethanol electro-oxidation mechanism by diminishing the adsorption strength of the poisoning intermediates (i.e CO) on the Pt sites and releasing the surface to promote new cycles of adsorption and electro-oxidation.

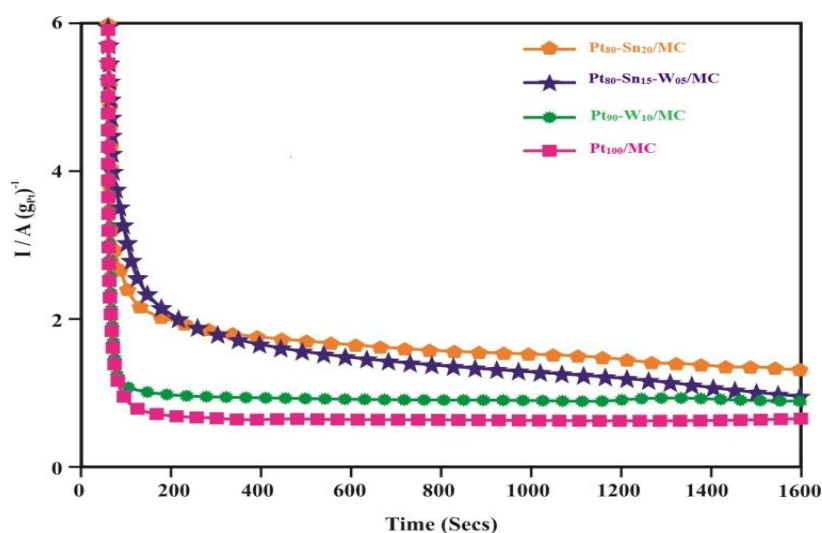


Figure 6: Chronoamperometry result of ethanol oxidation for Pt–Sn/MC (80:10), Pt–W/MC (90:10), Pt–Sn–W/MC (80:15:05) in 0.5M H₂SO₄ + 1.0 mL CH₃CH₂OH solution at normal temperature.

3.6 Single cell performance

The Pt/MC, Pt–Sn/MC, Pt–W/MC and Pt–Sn–W/MC catalysts were estimated as anode catalyst for EOR by single membraneless ethanol fuel cell [MLEFC]. The polarization and power density curves of different catalysts are presented in figure. Among the catalysts comparison of MLEFC performance is also shown in fig. The open circuit potential voltage of cells containing Pt–Sn–W/MC, Pt–Sn/MC, Pt–W/MC and Pt/MC catalysts are 783mV, 723mV, 455V and 400mV, respectively (Figure.). The OCV of Pt–Sn–W is the highest value, 780mV, which is higher than that of other catalysts. This indicates that pure Pt is more rapidly poisoned by CO than any other alloy catalyst and that the oxidation of adsorbed CO is enhanced by the second or third metal. In the case of PtSnW the overall performance is superior to that Pt–Sn/MC and Pt–W/MC. The power densities were also obtained from cell potential and current density values. Table is shown the power densities for mesoporous carbon supported Pt, Pt–W, Pt–Sn and Pt–Sn–W are 4.71, 10.07, 18.18 and 34.18 mW/cm², respectively. However obtained results suggested that the substitution of W for Pt–Sn assists in remove surfaces poisoned by CO and provides additional reaction sites for ethanol oxidation. In agreement with the cyclic voltammetry and chronoamperometry results, the Pt–Sn–W anode catalyst exhibits higher single cell performance than Pt–Sn/MC, Pt–W/MC and Pt/MC catalysts in the MLEFC tests.

Table 3: Summary of performance of single fuel cell tests using (2 mg cm⁻² catalyst loading, 40 wt% catalyst on carbon).

Anode Catalysts	Open circuit voltage (V)	Maximum power density (mW/cm ²)	Current density at maximum power density (mA/cm ²)
Pt/MC (100)	0.40	4.71	48.342
Pt–Sn/MC (80:20)	0.723	18.18	80.69
Pt–W/MC (90:10)	0.455	10.07	59.84
Pt–Sn–W/MC (80:15:05)	0.783	34.18	130.23

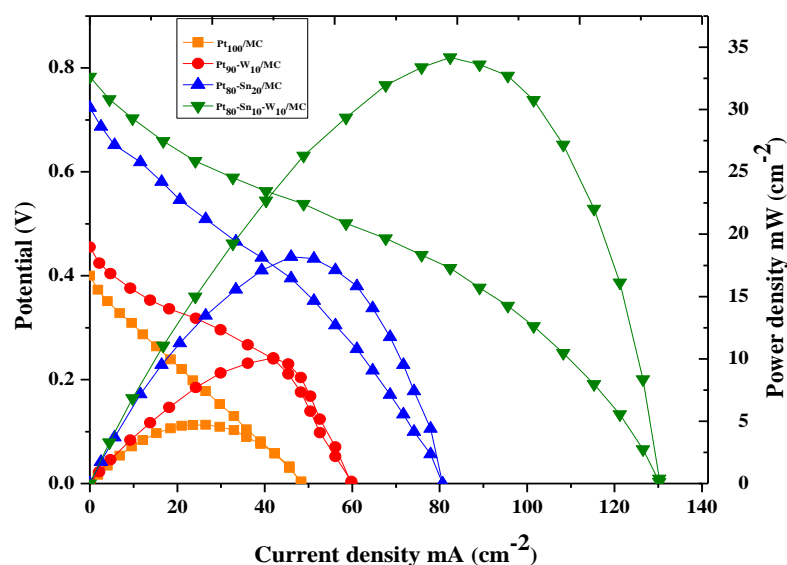


Figure 5: Polarization and power density cure of prepared catalysts for Pt/MC (100), Pt–Sn/MC (80:20), Pt–W/MC (90:10) and Pt–Sn–W/MC (80:15:05).

Conclusion

In this work, it is observed that the polymer precursor method process could be effectively used for the preparation of Pt/MC (100), Pt–Sn/MC (80:20), Pt–W/MC (90:10) and Pt–Sn–W/MC (80:15:05) electrocatalysts for ethanol oxidation. The X-ray diffractograms of the Pt–W/MC (90:10), Pt–Sn/MC (80:20) and Pt–Sn–W/MC (80:15:05) catalysts represented typical fcc structure of the Pt alloy peaks which shows that all the electrocatalysts resembles the phase disorder structure. In the case of Sn present in the Pt–Sn/MC (80:20) and Pt–Sn–W/MC (80:15:05) catalysts represented typical fcc structure of Pt alloys with the presence of tin oxide space. The physical characterization of TEM images represented the all the metal particles evenly dispersed in the mesoporous carbon supported. Additionally, particle size decrease binary catalysts of Pt–Sn/MC (80:20) and Pt–W/MC (90:10) to ternary Pt–Sn–W/MC (80:15:05) catalyst. EDX analysis indicated that the experimental composition is in agreement with the nominal composition of the catalyst, which confirm the formation Pt–Sn–W/MC, Pt–W/MC and Pt–Sn/MC metal catalysts having typical Pt crystalline structure and the formation of Pt–Sn alloy. The electrochemical characterization of CV found that mesoporous carbon supported ternary catalyst Pt–Sn–W/MC have higher current density and ethanol molecule oxidation started at lower onset potentials. It is due to the presence of W in the Pt–Sn surface which favors the activation interfacial water molecule. In this work, mesoporous carbon-supported ternary Pt–Sn–W/MC and binary Pt–Sn/MC and Pt–W/MC anode catalysts were successfully tested in a single membraneless fuel cell using 1.0 M ethanol as the fuel and 0.1 M sodium perborate as the oxidant in the presence of 0.5 M H₂SO₄ as the electrolyte. Among them Pt–Sn–W/MC ternary catalyst is given higher power density and current density. Electrochemical test and single cell test confirmed that Pt–Sn–W/MC (80:15:05) ternary catalysts is effective anode catalyst for membraneless ethanol fuel cell [MLEFC].

Acknowledgments-The financial support for this research from University Grants Commission (UGC), New Delhi, India through a Major Research Project 42-325/20134 (SR) is gratefully acknowledged.

References

1. Dyer C.K., *J. Power Sources*. 106 (2002) 31–34.
2. Song S., Tsiakaras P., *Applied Catalysis B: Environmental*. 63 (2006) 187-193.
3. Bentley J., Derby R., *Renewable Fuels Association*. (2002) 14.
4. Lamy C., *Journal of Power Sources*. 105 (2002) 283-296.
5. Shao M.H., Adzic R.R., *Electrochim. Acta*. 50(2005) 2415.

6. Davis S.C., Anderson-Teixeira K.J., DeLucia E.H., *Trends in Plant Science*. 14 (2009) 140-146.
7. Ribeiro J., dos Anjos D.M., Kokoh K.B., Coutanceau C., Legar J.M., Olivi P., de Andrade A.R., Tremiliosi-Filho G., *Electrochimica. Acta*. 52 (2007) 6997-7006.
8. Choi M., Han C., Kim I.T., An J.C., Lee J.J., Lee H.K., Shim., *Journal of Nanoscience and Nanotechnology*. 11(2011) 838-841.
9. Rousseau S., Coutanceau C., Lamy C., Legar J.M., *J. Power Sources*. 158 (2006)18.
10. Colmati F., Antolini E., Gonzalez E.R., *Electrochem. Soc.* 154 (2007) B39.
11. Li H., Sun G., Cao L., Jiang L., Xin Q., *Electrochim. Acta*. 52 (2007) 6622.
12. Lamy C., Belgsir E.M., Legar J.M., *J. Appl. Electrochem.* 31(2001)799.
13. Legar J.M., Rousseau S., Coutanceau C., Hahn F., Lamy C. *Electrochim. Acta*. 50(2005) 5118.
14. Watanabe M., Motoo S, *J. Electroanal.Chem.* 60 (1975) 275.
15. Crown A., Moracs IR., Wieckowski A. *J. Electroanal. Chem.* 500 (2001) 333.
16. Goetz M., Wendt H., *Electrochim. Acta*. 43 (1998) 3637.
17. Neto A.O., Perez J., Napporn W.T., Ticianelli E.A., Gonzalez E.R. *J. Braz Chem Soc.* 11(2000) 39.
18. Ribeiro J., dos Anjos D.M., Kokoh K.B., Coutanceau C., Legar J.M., Olivi P., de Andrade A.R., Tremiliosi-Filho G. *Electrochim. Acta*. 52 (2007) 6997.
19. Rao V., Simonov P., Savinova E., Plaksin G., Cherepanova S., Kryukova G. *J. Power Sources*. 145(2005)178-87.
20. Figueiredo J., Pereira M., Serp P., Kalck P., Samant P., Fernandes J., *Carbon*. 44 (2006) 2516-22.
21. Arbizzani C., Beninati S., Soavi F., Varzi A., Mastragostino M., *J. power sources*. 185(2008)615-20.
22. Pechini M.P., Adams N. US Patent, 3, (1967) 330,697:1 (1967).
23. Bönemann H., Brijoux W., Brinkmann R., Fretzen R., Jousen T., Köppler R., Korall B., Neiteler P., Richter J. *J. Mol. Catal.* 86 (1994) 129–177.
24. Kim H., You D., Yoon H., Joo S., Pak C., Chang H., *J. Power Sources*. 180(2008)724-32.
25. Ribeiro J., dos Anjos D.M., Kokoh K.B., Coutanceau C., Legar J.M., Olivi P., de Andrade A.R., Tremiliosi-Filho G., *Electrochim.Acta*. 52(2007) 6997.
26. Somorjai C.A., *Journal of Physical Chemistry*. 94 (1990) 1013.
27. Vielstich W., In: *Fuel cells: Modern process for the electrochemical production of energy*, Wiley-Interscience (1968).
28. Profeti L.P.R., Simoes F.C., Olivi P., Kokoh K.B., Coutanceau C., Legar J.M., Lamy C., *J. Power Sources* 158 (2006) 1195.
29. Ribeiro J., Alves P.D.P., de Andrade A.R., *J. Mater. Sci.* 42 (2007) 9293.

(2017) ; <http://www.jmaterenvironsci.com>